BMC Plant Biology

RESEARCH

Open Access

Integrated transcriptome and metabolome analysis provides insights into anthocyanin biosynthesis in *Cichorium intybus* L.

Mingzhao Zhu[1†], Ran Zhao[2,4†], Hanying Wu[3,4], Baohai Zhang[1], Bin Zhang[1] and Xiangyang Han[1*]

Abstract

Background Chicory is a unique and nutritious vegetable crop. However, the molecular mechanisms underlying anthocyanin biosynthesis in chicory remain poorly understood. We combined transcriptomics and metabolomics analyses to explore the molecular basis of anthocyanin biosynthesis in red-budded (Z1) and yellow-budded (Z7) chicory.

Results Integrated transcriptomics and metabolomics analyses were performed to investigate the molecular basis of anthocyanin biosynthesis in chicory. A total of 26 key structural genes, including *F3'H*, *DFR*, *CHS*, and *ANS*, were identified and enriched in pathways such as flavonoid and anthocyanin biosynthesis. Additionally, 29 transcription factors were identified, including 11 MYB, five bHLH, and two WD40 transcription factors, with seven *MYB* genes upregulated and four genes downregulated, indicating their roles in regulating anthocyanin biosynthesis. Notably, the MYB transcription factor, CI35997, which is homologous to RLL2A in lettuce, was predicted to positively regulate anthocyanin biosynthesis. Other transcription factors, such as AP2/ERF, bZIP, NAC, and Trihelix, have also been implicated. Metabolomics analysis revealed that cyanidin derivatives were the main contributors to the red coloration of chicory buds, with cyanidin-3-O-(6-O-malonyl)-glucoside being the most abundant. Furthermore, a competitive relationship between lignin and anthocyanin biosynthesis was observed, wherein the downregulation of lignin-related genes enhanced anthocyanin accumulation.

Conclusions This study identified key structural genes and transcription factors that offer molecular-level insights into anthocyanin biosynthesis in chicory. These findings provide valuable guidance for genetic improvement of chicory and other crops with high anthocyanin content.

Keywords *Cichorium intybus* L., Anthocyanin, Transcriptomics, Metabolome

†Mingzhao Zhu and Ran Zhao contributed equally to this work.

*Correspondence:
Xiangyang Han
hanxiangyang@nercv.org
[1]State Key Laboratory of Vegetable Biobreeding, Beijing Key Laboratory of Vegetable Germplasms Improvement, Key Laboratory of Biology and Genetics Improvement of Horticultural Crops (North China), Beijing Vegetable Research Center, National Engineering Research Center for Vegetables, Beijing Academy of Agricultural and Forestry Sciences, Beijing 100097, China
[2]State Key Laboratory of Plant Diversity and Specialty Crops, Institute of Botany, the Chinese Academy of Sciences, Beijing, China
[3]State Key Laboratory of Systematic and Evolutionary Botany, Institute of Botany, the Chinese Academy of Sciences, Beijing 100093, China
[4]China National Botanical Garden, Beijing, China

Background

Anthocyanins are secondary flavonoid metabolites that are widely found in plants and are characterized by a C6-C3-C6 carbon skeleton. In plants, anthocyanins typically exist in their glycosylated forms, with the most common aglycone types being cyanidin, delphinidin, pelargonidin, petunidin, malvidin, and peonidin. The structures of the substituents are the main basis for distinguishing anthocyanins [1]. Anthocyanins impart vibrant colors, such as red, orange, purple, and blue, to plant organs [2]. These colors strongly attract insects and other organisms, facilitating pollination and seed dispersal [3]. Anthocyanins also protect plants from pathogens, prevent photooxidative damage, and shield plants against biotic and abiotic stresses, enhancing plant stress resistance [4, 5]. The health benefits of anthocyanins have attracted increasing attention in recent years. Studies have shown that anthocyanins exhibit strong antioxidant activity, enhance the human defense system, reduce free radical damage, slow the progression of chronic diseases, prevent cardiovascular diseases and cancer, and delay aging [6–8]. Therefore, the effects of anthocyanins on plants and humans have become a key research focus.

Research on plant anthocyanin metabolic pathways is highly advanced. Anthocyanin biosynthesis is divided into three steps. The first stage begins with phenylalanine, which is sequentially catalyzed by phenylalanine ammonia-lyase (PAL), cinnamic acid 4-hydroxylase (C4H), and 4-coumarate-CoA ligase (4CL) to form 4-coumaroyl-CoA. In the second stage, 4-coumaroyl-CoA and malonyl-CoA are sequentially catalyzed by chalcone synthase (CHS), chalcone isomerase (CHI), and flavanone 3-hydroxylase (F3H) to form dihydrokaempferol. The third stage involves structural genes such as *flavanone 3'-hydroxylase* (*F3'H*), *dihydroflavonol 4-reductase* (*DFR*), and *anthocyanidin synthase* (*ANS*). DFR catalyzes the formation of colorless anthocyanidins, which are then converted to colored anthocyanins by ANS. Anthocyanins undergo acetylation, glycosylation, and methylation in the cytoplasm before being transported to vacuoles for storage [9].

The structural genes involved in anthocyanin synthesis in plants are regulated by control genes. Three main types of transcription factors regulate anthocyanin synthesis in plants: MYB, basic helix-loop-helix (bHLH), and WD40 repeat proteins [10]. In *Arabidopsis*, anthocyanin-regulating genes are divided into R2R3-MYB transcription factors and the MYB-bHLH-WD40 (MBW) complex. MYB11, MYB12, MYB75, MYB90, and MYB111 are among the earliest identified R2R3-MYB transcription factors, capable of activating genes such as *PAL*, *CHS*, *F3H*, and *DFR*. The MBW complex includes four R2R3-MYB protein-coding genes (*PAP1*, *PAP2*, *MYB113*, and *MYB114*), three bHLH protein-coding genes (*Transparent Testa 8*, *TT8*; *GLABRA3*, *GL3*; and *Enhancer of GLABRA3*, *EGL3*), and one WD40 repeat protein-coding gene (*Transparent Testa Glabra1*, *TTG1*). This complex primarily activates structural genes in the later stages of anthocyanin synthesis, such as *F3H*, *DFR*, and *ANS* [11–14]. Numerous transcription factors regulating anthocyanin synthesis have been identified in other dicotyledonous plants. In petunias, PhAN2 and PhAN4 activate *CHS* and *DFR* [15, 16], while ASR interacts with AN1 and AN11 to regulate anthocyanins via the MBW complex [17]. In grapes, VvMYBA2r positively regulates anthocyanin biosynthesis by forming the VvMYBA2r-VvMYCA1-VvWDR1 complex [18]. In apples, MdMYBA activates *MdANS* expression to promote anthocyanin accumulation. MdMYB10 requires the coexpression of two bHLH proteins, MdbHLH3 and MdbHLH33, to induce anthocyanin biosynthesis [19]. Several transcription factors repress anthocyanin synthesis. In *Arabidopsis*, MYB4 and its homologs MYB7 and MYB32 interact with bHLH transcription factors (TT8, GL3, and EGL3), disrupting the MBW complex and hindering anthocyanin synthesis [20]. Heterologous expression of *CmMYB1* from chrysanthemums inhibits flavonoid-related genes in *Arabidopsis* [21]. In poplars, MYB182 disrupts the transcriptional activation of MYB134, thereby inhibiting anthocyanin synthesis [22]. In contrast, the regulation of anthocyanins in monocotyledonous plants is relatively simple. In maize, the anthocyanin synthesis genes (*CHS*, *CHI*, *F3H*, *DFR*, *ANS*, and *UFGT*) are regulated solely by the MBW complex [23]. In lilies and orchids, MYB transcription factors predominantly regulate anthocyanin genes [24]. Li et al. (2022) identified a rare bHLH transcription factor in onions that interacts with AcMYB1 to coactivate *AcANS* and *AcF3H1* [25].

Chicory (*Cichorium intybus* L.) is a perennial herb belonging to the genus Cichorium in the family Asteraceae, which is cultivated worldwide. Forced chicory, a cultivated variety developed through specific methods to produce softer, lighter-colored leaves, originates from the Mediterranean, Central Asia, and North Africa and was introduced to China in the 1990s. It quickly gained popularity owing to its tender appearance, bittersweet taste, and crisp texture, earning the title of a noble vegetable. In traditional Chinese medicine, the aerial parts and roots of chicory are considered bitter and cold, respectively, with properties of clearing heat, promoting diuresis, and aiding digestion. Modern studies have shown that chicory is rich in dietary fiber, flavonoids, fatty acids, amino acids, sesquiterpene lactones, vitamins, minerals, and antioxidants, offering benefits like lipid regulation and anti-inflammatory and analgesic effects [26, 27]. Forced chicory is classified into yellow and red types based on the bud color. Few studies have reported chicory anthocyanins, and their synthetic mechanisms remain

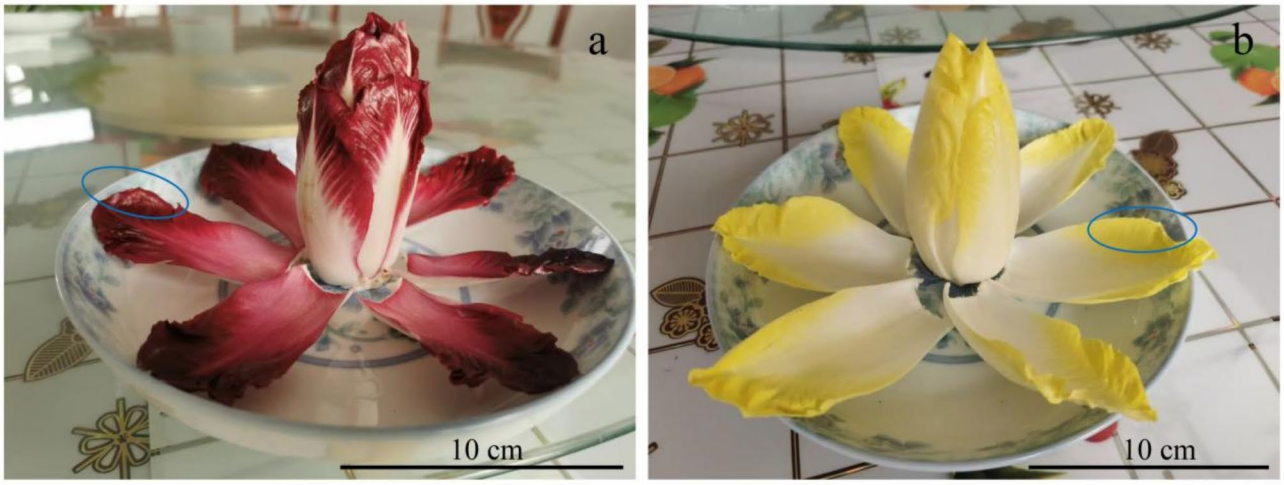

Fig. 1 The chicory materials used for this experiment. a, Z1 (red). b, Z7 (yellow). The blue circles indicate the sampling sites

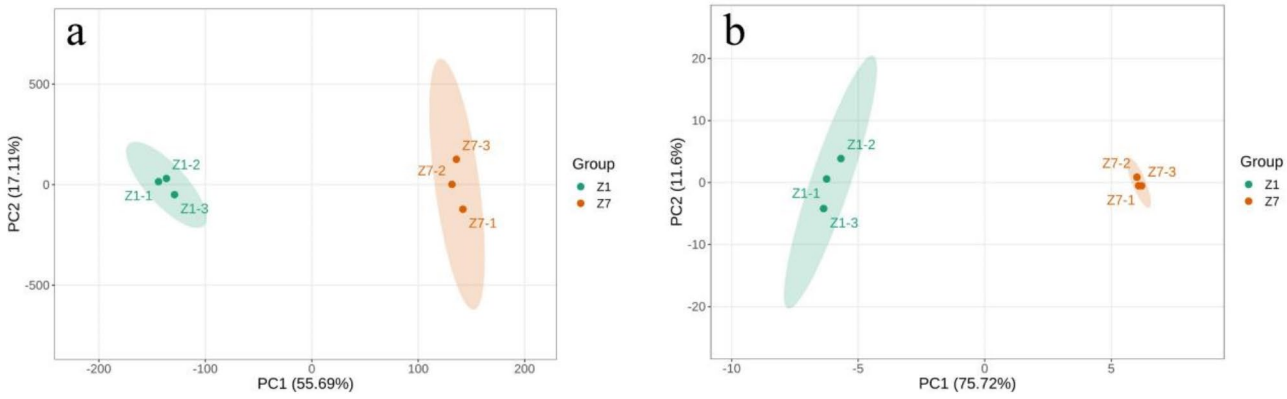

Fig. 2 Principal component analysis (PCA) results of transcriptomics data (**a**) and metabolomics data (**b**)

unknown. This study used red- and yellow-bud forced chicory (Fig. 1) to explore anthocyanin synthesis mechanisms via transcriptomics and metabolomics analyses, thereby providing a foundation for breeding high-quality varieties.

Results

Transcriptomics and metabolomics data analysis

Quality control results for the transcriptome data (Table S1) showed that after filtering, approximately 43.19 to 56.46 million clean reads were generated. The GC content ranged from 44.43 to 45.21%, and the Q30 ratio exceeded 93.99%, indicating that the sequencing data were of high quality and suitable for downstream analysis.

Principal component analysis (PCA) of the transcriptome and metabolome data showed clear separation between groups and tight clustering within groups, indicating the reliability and consistency of the anthocyanin-related datasets (Fig. 2).

Identification of anthocyanin composition

A noticeable color difference was observed between the two forced chicory materials, Z1 and Z7 (Fig. 1), which was speculated to result from anthocyanin accumulation. To explore this, a targeted metabolomics analysis of anthocyanins was performed, which identified 59 anthocyanin-related metabolites classified into seven subgroups: 56 anthocyanins, one procyanidin, and two other compounds. Of these, 58 metabolites were detected in Z1, 20 in Z7, and 19 were shared (Table S2). In addition, 11 differential metabolites were identified between Z1 and Z7, including four cyanidins, one delphinidin, one malvidin, two pelargonidins, two peonidins, and one flavonoid (Table 1). In Z7, cyanidin-3-O-(6”-O-malonyl) galactoside was not detected, and the contents of other components were minimal, with quercetin-3-O-glucoside being the highest at only 3.31 μg/g. In contrast, Z1 exhibited significantly higher anthocyanin content, with cyanidin-3-O-(6-O-malonyl-beta-D-glucoside) being the most abundant at 7,292.60 μg/g, accounting for 89.54% of the total anthocyanins (Fig. 3). This was followed by

Table 1 Content and statistical analysis of differential metabolites between Z1 and Z7 (μg/g)

Compounds	Class	Content (μg/g)		*p*-value	Log-$_2$FC
		Z1	Z7		
Cyanidin-3-O-(6″-O-malonyl)galactoside	Cyanidin	4.02	0.00	0.007	Inf
Cyanidin-3-O-(6-O-malonyl-beta-D-glucoside)	Cyanidin	7,292.60	2.15	0.002	11.73
Cyanidin-3-O-glucoside	Cyanidin	195.24	0.06	0.002	11.78
Cyanidin-3,5-O-diglucoside	Cyanidin	100.40	0.01	0.008	12.86
Delphinidin-3-O-(6″-O-acetyl)galactoside	Delphinidin	8.12	0.01	0.002	9.68
Malvidin-3-O-(6-O-malonyl-beta-D-glucoside)	Malvidin	2.61	0.03	0.002	6.29
Pelargonidin-3,5-O-diglucoside	Pelargonidin	1.72	0.07	0.000	4.69
Pelargonidin-3-O-glucoside	Pelargonidin	2.42	0.10	0.014	4.57
Peonidin-3-O-glucoside	Peonidin	6.74	0.13	0.068	5.66
Peonidin-3,5-O-diglucoside	Peonidin	2.96	0.17	0.087	4.15
Quercetin-3-O-glucoside	Flavonoid	527.65	3.31	0.002	7.31

quercetin-3-O-glucoside at 527.65 μg/g (6.48%). Cyanidin-3-O-glucoside and cyanidin-3,5-O-diglucoside were also relatively abundant, measured at 195.24 μg/g (2.40%) and 100.40 μg/g (1.23%), respectively. The remaining components were present in much lower amounts, with none exceeding 10 μg/g.

Differentially expressed gene identification and enrichment analysis

The analysis identified 3,888 differentially expressed genes (DEGs) between Z1 and Z7, including 2,345 upregulated and 1,543 downregulated genes (Fig. S1). Kyoto Encyclopedia of Genes and Genomes (KEGG) enrichment analysis of these DEGs showed that the top 50 enriched pathways were predominantly related to metabolic processes, with 407 genes involved in metabolic pathways and 287 genes involved in secondary metabolite biosynthesis. Furthermore, 97 genes were enriched in the plant-pathogen interaction pathway. Specifically, in pathways associated with anthocyanin metabolism, 17 genes were enriched in flavonoid biosynthesis, whereas the anthocyanin biosynthesis and flavone and flavonol biosynthesis pathways each contained three enriched genes (Fig. 4).

Identification of key DEGs related to anthocyanin metabolism

Based on the KEGG enrichment analysis of DEGs, we identified 26 key genes associated with anthocyanin metabolism, including flavonoid biosynthesis, anthocyanin biosynthesis, flavonol biosynthesis, and secondary metabolite biosynthesis pathways. Among these, four genes were downregulated, whereas the others were upregulated (Fig. 5; Table S3). Specifically, these genes included three encoding F3'H [EC:1.14.14.82], two encoding anthocyanin 5-O-glucoside-6‴-O-malonyltransferase (5MaT) [EC:2.3.1.172], one encoding anthocyanidin 3-O-glucoside 6″-O-acyltransferase (3-GAT) [EC:2.3.1.215], two encoding DFR [EC:1.1.1.219, 1.1.1.234], one encoding CHS [EC:2.3.1.74], one encoding ANS [EC:1.14.20.4], two encoding CHI [EC:5.5.1.6], three encoding caffeoyl-CoA O-methyltransferase (CCoAOMT) [EC:2.1.1.104], four encoding PAL [EC:4.3.1.24], three encoding 4CL [EC:6.2.1.12], one encoding F3H [EC:1.14.11.9], one encoding flavonol synthase (FLS) [EC:1.14.20.6], and two encoding anthocyanidin 3-O-glucosyltransferase (3-GT) [EC:2.4.1.115]. In addition to structural genes, transcription factors directly or indirectly involved in anthocyanin metabolism were identified among all the DEGs based on the gene annotation results. By integrating transcriptomics and metabolomics data through analyses such as the nine-quadrant plot (Fig. S2) and a correlation heatmap (Fig. S3), we identified 29 transcription factors, including 11 MYB, five bHLH, two WD40, three AP2/ERF-ERF, four bZIP, one NAC, two SNF2, and one Trihelix transcription factor (Table S3).

Quantitative reverse transcriptase-polymerase chain reaction validation

To validate the reliability of the RNA sequencing (RNA-seq) results, the ten key DEGs identified earlier were selected for verification by quantitative reverse transcriptase-polymerase chain reaction (qRT-PCR). qRT-PCR analysis demonstrated that the relative expression levels of these genes in Z1 and Z7 were consistent with the trends observed in the RNA-seq data (Fig. 6).

The regulatory network of anthocyanin metabolism in Chicory

Based on the analysis of the key DEGs and differential metabolites, a model diagram of anthocyanin biosynthesis in chicory was established. As shown in Fig. 7, the flavonoid metabolic pathway was abnormally active in Z1 than in Z7, with most structural genes in this pathway being upregulated. Starting from phenylalanine, the pathway progresses through key intermediates, such as dihydrokaempferol and dihydroquercetin, leading to the formation, modification, and stabilization of both

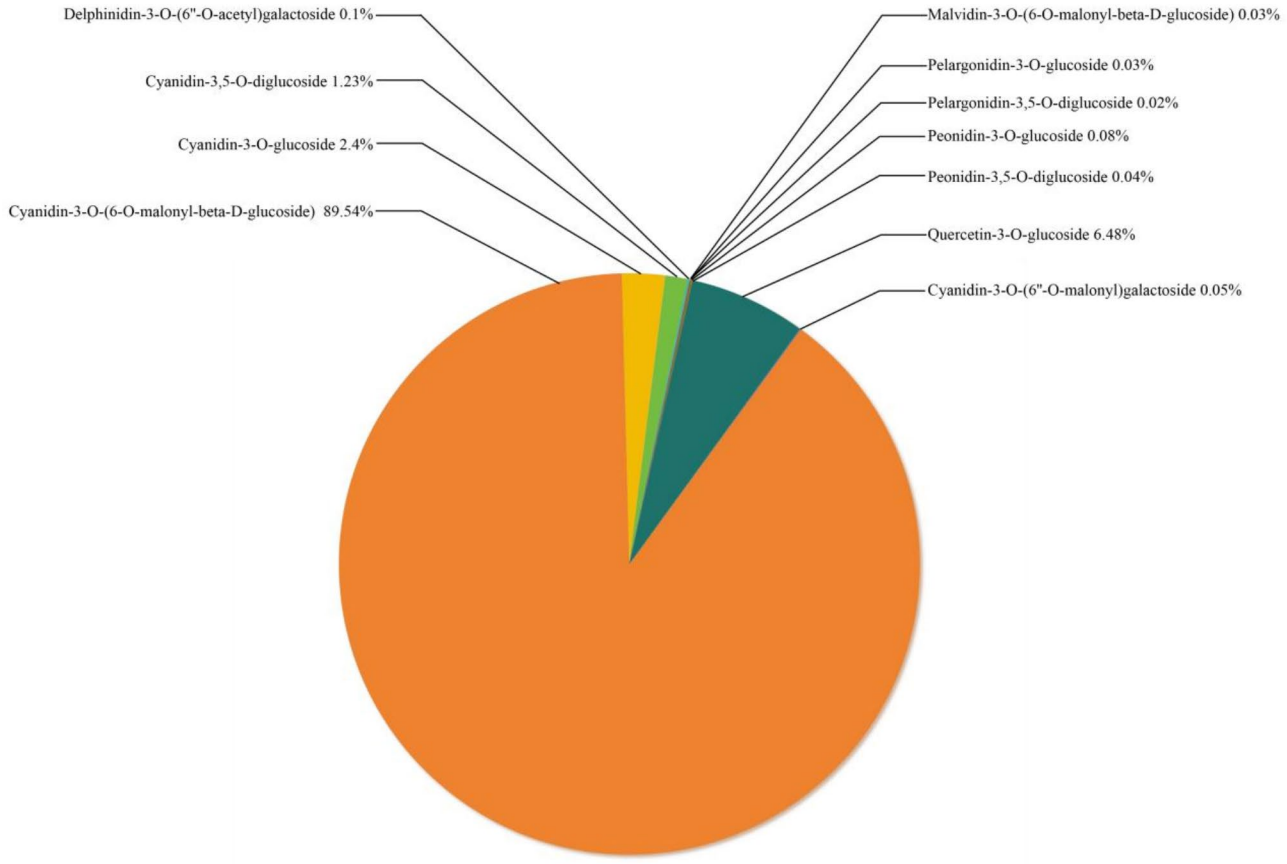

Fig. 3 The proportions of individual anthocyanins in Z1 among the differential anthocyanin metabolites

colorless and colored anthocyanins. Enzymes at each stage exhibited increased activity, collectively contributing to the red trait in Z1 buds, which aligned closely with our metabolomics analysis results. Notably, the downregulation of *FLS* also promoted anthocyanin accumulation because FLS competes with DFR for the same catalytic substrate [28]. Reduced FLS activity diverts upstream metabolites toward anthocyanin biosynthesis. However, the quercetin-3-O-glucoside content in Z1 remained significantly higher than that in Z7, likely because of the overproduction of upstream metabolites. Even with reduced *FLS* expression, a small fraction of these metabolites was directed toward the quercetin branch, resulting in substantial quercetin-3-O-glucoside accumulation, although the exact mechanisms require further investigation. Additionally, the lignin metabolic pathway, a branch of the phenylpropanoid metabolic pathway, competes with anthocyanin biosynthesis. At the branching point, 4-coumaroyl-CoA is sequentially catalyzed by p-coumaroyl-CoA 3-hydroxylase (C3H) and CCoAOMT before lignin synthesis begins [29]. Downregulation of *CCoAOMT* expression in Z1 further promoted anthocyanin accumulation by reducing the flux toward lignin biosynthesis.

Discussion

The effect of differential anthocyanins in the two Chicory materials on bud color

Anthocyanin content is widely recognized as the primary factor responsible for the vibrant coloration of plant organs. However, the formation of red buds in chicory and the mechanisms underlying anthocyanin synthesis remain largely unexplored. Previous studies have highlighted the roles of cyanidin derivatives in plant coloration. For example, high levels of cyanidin derivatives have been identified as key determinants of purple rind traits in sugarcane [30]. Similarly, delphinidin 3-O-glucoside and delphinidin 3-O-rutinoside were significantly enriched in purple peppers than in green peppers [31]. In roses, seven anthocyanins were significantly enriched in deep pink petals than in light pink petals [32]. Likewise, in *Michelia maudiae*, the red-flowered mutant exhibited a 157-fold increase in anthocyanins, including peonidin O-hexoside, cyanidin O-syringic acid, cyanidin 3,5-O-diglucoside, cyanidin 3-O-glucoside, and pelargonidin 3-O-glucoside, in comparison with the white-flowered mutant [33]. In this study, cyanidin derivatives were identified as the primary differential anthocyanin metabolites between Z1 and Z7, accounting for 93.22% of the

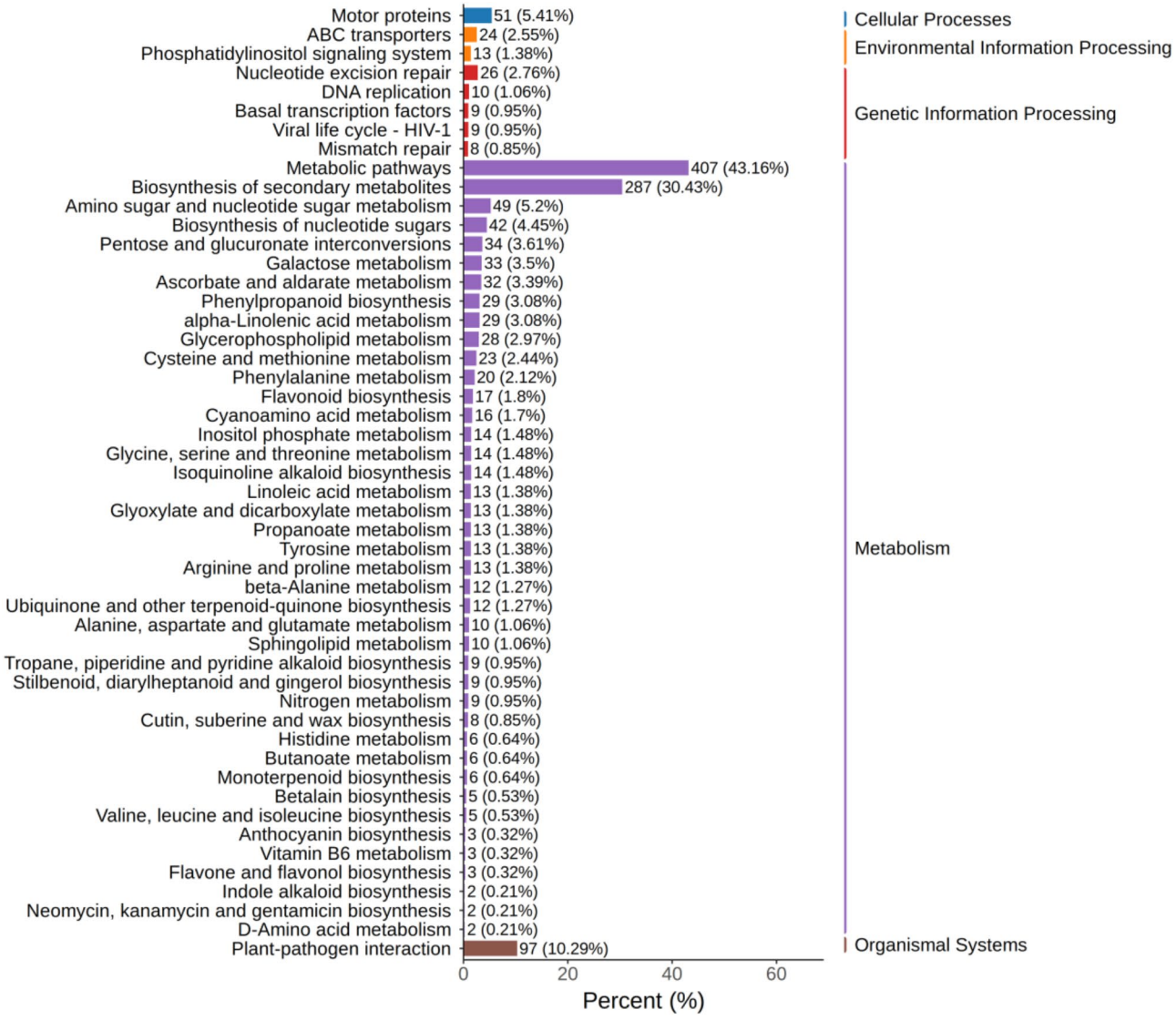

Fig. 4 Kyoto Encyclopedia of Genes and Genomes (KEGG) enrichment analysis of differentially expressed genes (DEGs)

total anthocyanin content. Among these, cyanidin-3-O-(6-O-malonyl-beta-D-glucoside) showed an absolute content of 7292.6 μg/g. These findings suggest that cyanidin derivatives are key factors driving the formation of red buds in chicory.

The transcription factors regulating anthocyanin metabolism in Chicory

Anthocyanin biosynthesis is a branch of the flavonoid metabolic pathway originating from phenylalanine. Through a series of enzymatic reactions, including glycosylation, methylation, and acylation, anthocyanins are transported to and accumulate in vacuoles, with multiple key enzymes involved in their synthesis and modification (Fig. 7) [34]. In addition to structural genes, transcription factors are critical regulators of anthocyanin metabolism. Among these, MYB transcription factors are the most common and typically form complexes with bHLH and WD40 proteins to jointly regulate anthocyanin biosynthesis. MYB is a key component of the MBW complex and not only activates the proanthocyanin metabolic pathway but can also independently initiate this pathway. As a central and dominant regulator of anthocyanin metabolism and pigmentation patterns in plants, MYB is often referred to as the master regulator. MYB transcription factors function as both positive and negative regulators. In this study, integrated transcriptomics and metabolomics analyses combined with a nine-quadrant diagram analysis identified seven upregulated and four downregulated MYB genes. The upregulated genes were likely involved in the positive regulation of anthocyanin biosynthesis, whereas the downregulated genes may contribute to its negative regulation. Notably, CI35997 is homologous to the transcription factor RLL2A in lettuce,

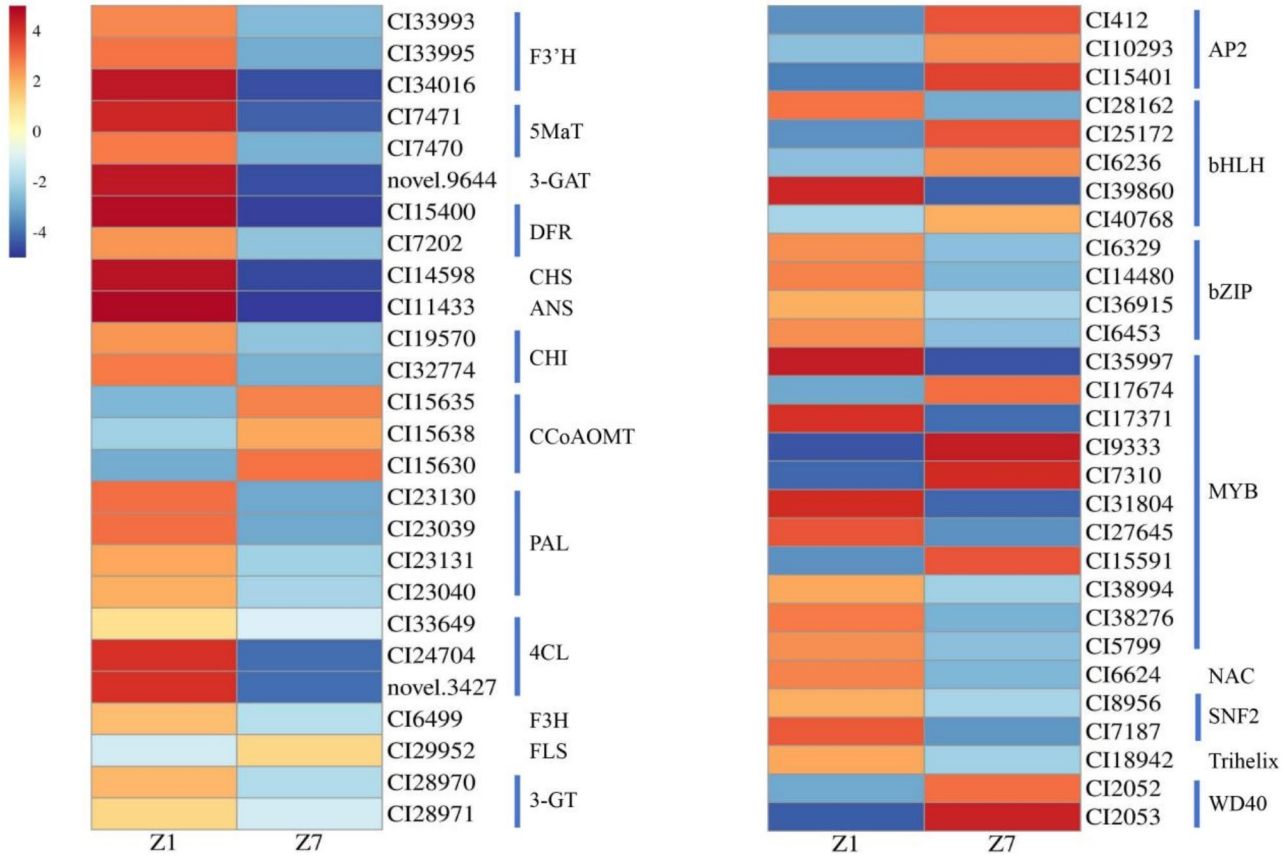

Fig. 5 Heatmap showing the expression levels of key genes related to anthocyanin metabolism. The color gradient represents gene expression levels (blue: low, red: high), with expression data log_2-transformed

which has been shown to positively regulate anthocyanin biosynthesis in lettuce [35]. This finding supports the predicted regulatory roles of MYB transcription factors, although the functions of the remaining genes require further validation.

In addition to the well-known transcription factors MYB, bHLH, and WD40, which regulate anthocyanin metabolism, we identified several other transcription factors that may be associated with anthocyanin metabolism, including AP2/ERF-ERF, bZIP, NAC, SNF2, and Trihelix. The overexpression of the AP2/ERF transcription factor in *Arabidopsis* under phosphorus-deficient conditions results in reduced anthocyanin accumulation [36]. This suggests that AP2/ERF acts as a negative regulator of anthocyanin metabolism. Similarly, in the present study, we identified three downregulated AP2/ERF-ERF transcription factors in chicory that are likely to play similar negative regulatory roles in anthocyanin biosynthesis. In contrast, the bZIP transcription factor family has been shown to positively regulate anthocyanin metabolism in several plant species. For example, in tomatoes, HY5 directly binds to the promoters of anthocyanin biosynthesis genes, such as CHS and DFR, to promote anthocyanin synthesis [37]. In apples, MdbZIP44 enhances MdMYB1 binding to the promoters of downstream target genes in response to ABA, thereby promoting anthocyanin accumulation [38]. Consistent with these findings, we identified four upregulated bZIP transcription factors in chicory that may positively regulate anthocyanin metabolism. The NAC transcription factor family is another important regulator of anthocyanin biosynthesis, often acting upstream of the MYB transcription factors. Previous studies have demonstrated the role of NAC in regulating anthocyanin metabolism in various plants [39–41]. In the present study, we identified an upregulated NAC transcription factor in chicory that may play a crucial role in the activation of anthocyanin biosynthesis. The Trihelix transcription factor family has been implicated in the regulation of anthocyanins. Meng et al. (2024) conducted transcriptome and metabolome analyses of two differently colored sepals of *Aquilegia oxysepala* and identified a series of transcription factors associated with anthocyanin metabolism, including bHLH, Trihelix, MYB, and NAC [42]. Consistent with these findings, we identified an upregulated Trihelix transcription factor in chicory that may also contribute to anthocyanin biosynthesis. Recent studies have highlighted the role of chromatin remodeling in the

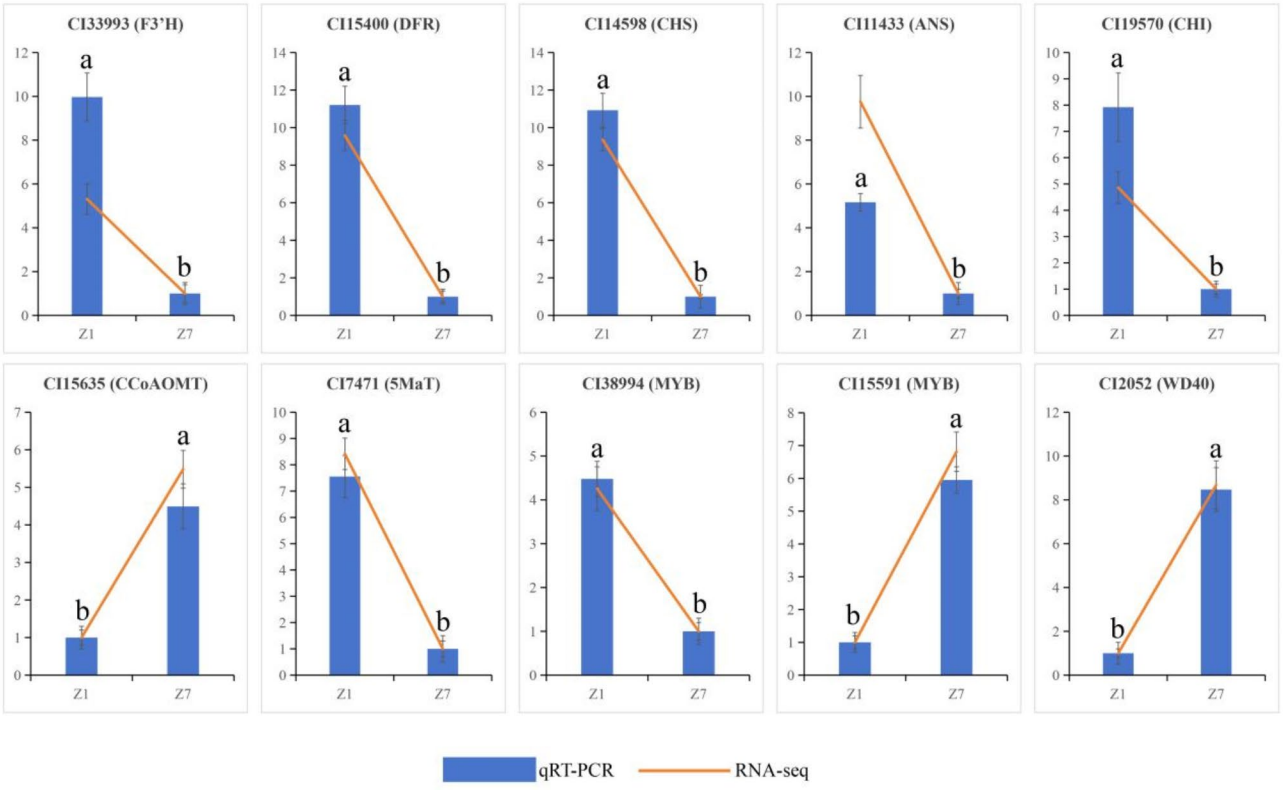

Fig. 6 Validation of RNA sequencing (RNA-seq) data using quantitative reverse transcriptase-polymerase chain reaction (qRT-PCR) for 10 differentially expressed genes (DEGs). The y-axis represents the $\log_2$-transformed fold-change in gene expression levels, calculated relative to Z7 as the control group. Different letters (a, b) above the bars indicate significant differences ($P < 0.05$) between Z1 and Z7

regulation of anthocyanin biosynthesis. Cai et al. (2021) demonstrated that the chromatin-remodeling complex SWI2/SNF2-Related 1 interacts with H3K4me3 to regulate anthocyanin biosynthesis [43]. On the basis of these findings, we speculated that the SNF2 transcription factor identified in this study may also be involved in the regulation of anthocyanin biosynthesis in chicory.

Conclusions

This study explored the synthesis and accumulation patterns of anthocyanins during the formation of red buds in chicory using transcriptomics and metabolomics analyses. The results showed that cyanidin derivatives contributed 93.22% to the red color of red-bud chicory, with cyanidin-3-O-(6-O-malonyl-beta-D-glucoside) being the predominant component. In the anthocyanin metabolic pathway, structural genes such as *DFR*, *ANS*, and *F3'H* were significantly upregulated, while *FLS* was downregulated, reducing substrate competition and promoting anthocyanin accumulation. In addition, 29 transcription factors related to anthocyanin metabolism were identified, including MYB, bHLH, WD40, AP2/ERF, bZIP, NAC, SNF2, and Trihelix, with MYB, bHLH, and WD40 being the key regulatory factors. The study also revealed a competitive relationship between anthocyanin and lignin metabolic pathways, where the downregulation of lignin-related genes (e.g., CCoAOMT) facilitated metabolic flux toward anthocyanin synthesis. This study provides new insights into the molecular basis of red-bud formation in chicory and offers a theoretical reference for improving the color and nutritional value of chicory varieties.

Methods

Plant materials and sampling

On July 16, 2023, direct seeding of chicory began in the open fields. Following a period of growth and care, efforts were made to ensure full root development. Root harvesting began on November 5, 2023, with the goal of achieving root maturity. Forcing began on December 5, 2023, in a completely dark artificial climate chamber to promote bud growth. The soft cultivation environment was maintained at a temperature of 15℃–18℃ and a humidity level of 85–95%. After approximately one month of soft cultivation, the chicory buds grew to approximately 10 cm, and a harvest survey was conducted on January 4, 2024.

Ruanhong No. 1 and FIRST LADY were used in this study. Ruanhong No. 1 was developed by the Beijing Vegetable Research Center, whereas the seeds of FIRST LADY were introduced by the Dutch company Chicosem

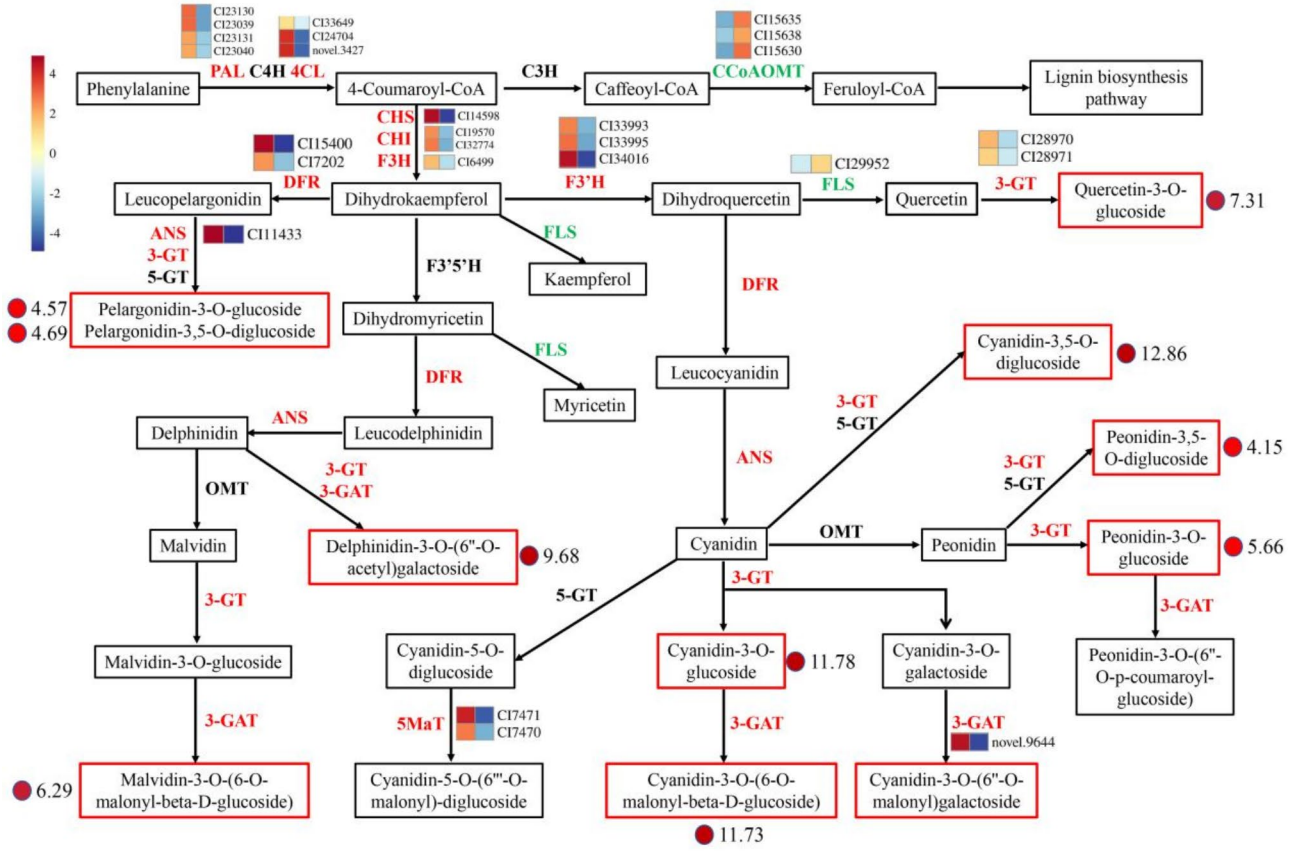

Fig. 7 Metabolomics and transcriptomics analyses of flavonoid biosynthesis and related pathways in forced chicory. Upregulated metabolites are highlighted in red boxes; upregulated enzymes are shown in red font; and downregulated enzymes are shown in green font. Colored squares represent gene expression levels (left: Z1; right: Z7), with expression data $\log_2$-transformed. The red circles indicate the fold-change in metabolite levels, reflecting the relative change in Z1 in comparison with Z7, with the data $\log_2$-transformed. PAL: phenylalanine ammonia-lyase; C4H: cinnamic acid 4-hydroxylase; 4CL: 4-coumarate-CoA ligase; CHS: chalcone synthase; CHI: chalcone isomerase; F3H: flavanone 3-hydroxylase; C3H: p-Coumaroyl-CoA 3-hydroxylase; CCoAOMT: caffeoyl-CoA O-methyltransferase; F3'H: flavanone 3'-hydroxylase; F3'5'H: flavanone 3'5'-hydroxylase; DFR: dihydroflavonol 4-reductase; FLS: flavonol synthase; ANS: anthocyanidin synthesis; 3-GT: anthocyanidin 3-O-glucosyltransferase; 5-GT: anthocyanidin 5-O-glucosyltransferase; OMT: O-methyltransferase; 5MaT: anthocyanin 5-O-glucoside-6‴-O-malonyltransferase; 3-GAT: anthocyanidin 3-O-glucoside 6″-O-acyltransferase

BV. After being forced, the leaves of Ruanhong No. 1 turned red, whereas those of FIRST LADY turned yellow. In this experiment, they were designated as Z1 and Z7, respectively (Fig. 1). The leaves were divided into two parts: the part near the base of the leaf was white, whereas the leaf margins and area near the tip were yellow or red. During sampling, we collected the red and yellow parts of the leaf margins from Z1 and Z7 for anthocyanin content detection and RNA sequencing. The experiment was conducted in triplicate, each consisting of six individual plants. The three samples for Z1 were labeled Z1-1, Z1-2, and Z1-3, while the three samples for Z7 were labeled Z7-1, Z7-2, and Z7-3. The samples were sent to Wuhan Metware Biotechnology Co. Ltd. (Wuhan, China) for metabolomics and transcriptomics sequencing.

Anthocyanin extraction and component analysis

The samples were freeze-dried and ground into a fine powder. A 50-mg aliquot of the powder was extracted using 0.5 mL of a methanol/water/hydrochloric acid solution (500:500:1, V/V/V). The extract was vortexed for 5 min, ultrasonicated for 5 min, and centrifuged at 12,000 × *g* at 4 °C for 3 min. The residue was then subjected to a second extraction step under identical conditions. The combined supernatants were filtered through a 0.22-μm membrane filter (Anpel) prior to liquid chromatography-tandem mass spectrometry (LC-MS/MS) analysis. The extracts were analyzed using a ultra-high performance liquid chromatography (UPLC)-electrospray ionization (ESI)-MS/MS system, consisting of a UPLC system (ExionLC™ AD; https://sciex.com.cn/) coupled with MS (Applied Biosystems 6500 Triple Quadrupole; https://sciex.com.cn/). The analytical conditions were as follows: a Waters ACQUITY BEH C18 column was used with a solvent system consisting of water with 0.1% formic acid

(solvent A) and methanol with 0.1% formic acid (solvent B). The gradient program began at 95:5 V/V (A: B) at 0 min, shifted to 50:50 V/V at 6 min, 5:95 V/V at 12 min, held for 2 min, reverted to 95:5 V/V at 14 min, and held for another 2 min. The flow rate was set at 0.35 mL/min, the column temperature was maintained at 40 °C, and the injection volume was 2 μL.

Linear ion trap (LIT) and triple quadrupole (QQQ) scans were conducted using a QTRAP® 6500 + LC-MS/MS System, a triple quadrupole-linear ion trap mass spectrometer equipped with an ESI Turbo Ion-Spray interface. The system operated in positive-ion mode and was managed using Analyst 1.6.3 software (Sciex). The ESI source parameters were set as follows: ion source mode, ESI+; source temperature, 550 °C; ion-spray voltage, 5500 V; and curtain gas pressure, 35 psi. In total, 413 anthocyanin compounds were targeted for detection. Anthocyanins were analyzed using scheduled multiple reaction monitoring (MRM). Data acquisition was performed using Analyst 1.6.3 software, and metabolite quantification was performed using Multiquant 3.0.3 software (Sciex). Mass spectrometry parameters, including the declustering potentials (DPs) and collision energies (CEs) for individual MRM transitions, were further optimized. A specific set of MRM transitions was monitored for each period corresponding to the metabolites eluted at that time.

RNA extraction and sequencing and data analysis

Leaves used for RNA extraction were the same as those used for anthocyanin extraction. Total RNA was extracted using a FastPure Universal Plant Total RNA Isolation Kit (Vazyme Biotech Co., Ltd.) in accordance with the manufacturer's instructions. RNA quality and integrity were evaluated using an Agilent 2100 Bioanalyzer (Agilent Technologies, Santa Clara, CA, USA). RNA samples were selected for library preparation based on the following criteria: RIN ≥ 7.0, 28 S:18 S ratio ≥ 1.0, OD260/230 ≥ 2.0, and OD260/280 within the range of 1.8–2.2. cDNA libraries were constructed using a HiScript III All-in-one RT SuperMix kit (Vazyme Biotech Co., Ltd.) in accordance with the manufacturer's protocol. The six cDNA libraries were sequenced on an Illumina NovaSeq 6000 platform (Illumina, San Diego, CA, USA) with a read length of 150 bp. The transcriptome sequencing data volumes averaged 6 Gb/sample. To ensure data quality, low-quality reads were removed, including those containing adaptors, reads with more than 5% unknown nucleotides, or reads with Q20 scores < 20% (indicating a sequencing error rate of > 1%). The resulting high-quality reads were aligned to the *Cichorium intybus* reference genome [44] using Tophat2. The alignment files in the BAM/SAM format were further processed to remove duplicate reads. Gene expression levels were quantified using fragments per kilobase of exon per million mapped reads (FPKM) calculated using Cufflinks software.

The DEGs and differential metabolites were identified using Z7 as the reference. DEGs and significantly regulated metabolites were determined based on a threshold of|log2Fold Change| ≥ 2. Additionally, differential metabolites with absolute contents less than 1 μg/g were excluded from the analysis. Correlation analysis was performed to assess the consistency between biological replicates, and PCA was used to visualize the differences between sample groups. An enrichment analysis was performed using a hypergeometric test. Pathway-based enrichment was performed using KEGG, while gene ontology (GO) term-based analysis was used for GO enrichment. The correlation between genes and metabolites was analyzed using the "cor" function in R to calculate the Pearson correlation coefficient. A correlation coefficient with an absolute value greater than 0.8 and p-value less than 0.05 was considered significant. The fold changes in the genes and metabolites corresponding to these significant relationships were visualized using a nine-quadrant diagram and correlation network diagram.

Validation by quantitative real-time PCR

RNA sequencing (RNA-seq) results of DEGs between Z1 and Z7 were validated through quantitative real-time PCR (RT-qPCR) analysis of 10 genes potentially involved in anthocyanin synthesis. Gene-specific primers (Table S4) were designed using Premier 5 software, with actin (GenBank accession number EF528575) as the internal control [45]. The 20-μL PCR reaction mixture consisted of 1 μL of cDNA, 1 μL of each forward and reverse primer (10 μM), 10 μL of 2× Taq Pro Universal SYBR qPCR Master Mix (Vazyme Biotech Co., Ltd), and 7 μL of double-distilled water. The amplification protocol included an initial denaturation step at 95 °C for 30 s, followed by 40 cycles of 95 °C for 5 s, 60 °C for 15 s, and 72 °C for 20 s, performed on a Bio-Rad CFX96 Real-Time PCR System (Bio-Rad, USA). Each qPCR experiment was conducted in triplicate to ensure technical reproducibility. Relative gene expression levels were determined using the $2^{-\Delta\Delta CT}$ method. Using SPSS software, an independent-sample t-test was performed on the qRT-PCR results to compare the gene expression levels between Z1 and Z7, and to conduct a significance analysis. Prior to the t-test, normality (Shapiro-Wilk test) and homogeneity of variance (Levene's test) were assessed to ensure that the data met the assumptions of the t-test. The significance level was set at $P < 0.05$.

Abbreviations

bHLH	Helix-Loop-Helix
KEGG	Kyoto Encyclopedia of Genes and Genomes
GO	Gene Ontology
PCA	Principal Component Analysis

DEGs	Differentially Expressed Genes
PAL	Phenylalanine Ammonia-Lyase
C4H	Cinnamic acid 4-Hydroxylase
4CL	4-Coumarate-CoA Ligase
CHS	Chalcone Synthase
CHI	Chalcone Isomerase
F3H	Flavanone 3-Hydroxylase
C3H	p-Coumaroyl-CoA 3-Hydroxylase
CCoAOMT	Caffeoyl-CoA O-methyltransferase
F3'H	Flavanone 3'-Hydroxylase
F3'5'H	Flavanone 3'5'-Hydroxylase
DFR	Dihydroflavonol 4-Reductase
FLS	Flavonol Synthase
ANS	Anthocyanidin Synthesis
3-GT	Anthocyanidin 3-O-Glucosyltransferase
5-GT	Anthocyanidin 5-O-Glucosyltransferase
OMT	O-Methyltransferase
5MaT	Anthocyanin 5-O-Glucoside-6'''-O-malonyltransferase
3-GAT	Anthocyanidin 3-O-Glucoside 6''-O-acyltransferase

Supplementary Information

The online version contains supplementary material available at https://doi.org/10.1186/s12870-025-06393-1.

Supplementary Material 1

Supplementary Material 2

Supplementary Material 3

Supplementary Material 4

Supplementary Material 5

Supplementary Material 6

Supplementary Material 7

Supplementary Material 8

Author contributions

M.Z: Visualization, Validation, Software, Methodology, Formal analysis, Writing–original draft; R.Z: Conceptualization, Software; H.W: Writing–review and editing; B.Z (Baohai Zhang): Data curation; B.Z (Bin Zhang): Investigation; X.H: Resources, Funding acquisition, Conceptualization, Writing–review and editing. All authors have read and agreed to the published version of the manuscript.

Funding

This research was funded by the Scientific and technological innovation capacity building project of Beijing Academy of Agricultural and Forestry Sciences and Innovation and Development Program of Beijing Vegetable Research Center (KYCX202302) and the Scientific and Technological Innovation Capacity Building Project of BAAFS (KJCX20230126).

Data availability

The datasets generated and/or analysed during the current study are available in the SRA repository, https://www.ncbi.nlm.nih.gov/sra/PRJNA1198617.

Declarations

Ethics approval and consent to participate

Not applicable.

Consent for publication

Not applicable.

Competing interests

The authors declare no competing interests.

Received: 5 December 2024 / Accepted: 12 March 2025

Published online: 01 April 2025

References

1. Kong JM, Chia LS, Goh NK, Chia TF, Brouillard R. Analysis and biological activities of anthocyanins. Phytochemistry. 2003;64(5):923–33.
2. Kähkönen MP, Heinonen M. Antioxidant activity of anthocyanins and their Aglycons. J Agric Food Chem. 2003;51(3):628–33.
3. Narbona E, del Valle JC, Arista M, Buide ML, Ortiz PL. Major flower pigments originate different colour signals to pollinators. Front Ecol Evol. 2021;9:743850.
4. Naing AH, Kim CK. Abiotic stress–induced anthocyanins in plants: their role in tolerance to abiotic stresses. Physiol Plant. 2021;172(3):1711–23.
5. Lu Z, Wang X, Lin X, Mostafa S, Zou H, Wang L, Jin B. Plant anthocyanins: classification, biosynthesis, regulation, bioactivity, and health benefits. Plant Physiol Biochem. 2024;217:109268.
6. Bars-Cortina D, Sakhawat A, Piñol-Felis C, Motilva MJ. Chemopreventive effects of anthocyanins on colorectal and breast cancer: A review. Semin Cancer Biol. 2021. Academic Press.
7. Gonçalves AC, Nunes AR, Falcão A, Alves G, Silva LR. Dietary effects of anthocyanins in human health: A comprehensive review. Pharmaceuticals. 2021;14(7):690.
8. Mozos I, Flangea C, Vlad DC, Gug C, Mozos C, Stoian D, Luca CT, Horbańczuk JO, Horbańczuk OK, Atanasov AG. Effects of anthocyanins on vascular health. Biomolecules. 2021;11(6):811.
9. Cheng J, Wei G, Zhou H, Gu C, Vimolmangkang S, Liao L, Han Y. Unraveling the mechanism underlying the glycosylation and methylation of anthocyanins in Peach. Plant Physiol. 2014;166(2):1044–58.
10. Zhao L, Gao L, Wang H, Chen X, Wang Y, Yang H, Wei C, Wan X, Xia T. The R2R3-MYB, bHLH, WD40, and related transcription factors in flavonoid biosynthesis. Funct Integr Genom. 2013;13:75–98.
11. Albert NW, Davies KM, Lewis DH, Zhang H, Montefiori M, Brendolise C, Schwinn KE. A conserved network of transcriptional activators and repressors regulates anthocyanin pigmentation in eudicots. Plant Cell. 2014;26(3):962–80.
12. Gonzalez A, Zhao M, Leavitt JM, Lloyd AM. Regulation of the anthocyanin biosynthetic pathway by the TTG1/bHLH/Myb transcriptional complex in Arabidopsis seedlings. Plant J. 2008;53(5):814–27.
13. Koes R, Verweij W, Quattrocchio F. Flavonoids: a colorful model for the regulation and evolution of biochemical pathways. Trends Plant Sci. 2005;10(5):236–42.
14. Stracke R, Ishihara H, Huep G, Barsch A, Mehrtens F, Niehaus K, Weisshaar B. Differential regulation of closely related R2R3-MYB transcription factors controls flavonol accumulation in different parts of the *Arabidopsis Thaliana* seedling. Plant J. 2007;50(4):660–77.
15. Albert NW, Lewis DH, Zhang H, Irving LJ, Jameson PE, Davies KM. Light-induced vegetative anthocyanin pigmentation in Petunia. J Exp Bot. 2009;60(7):2191–202.
16. Quattrocchio F, Wing JF, Leppen HT, Mol JN, Koes RE. Regulatory genes controlling anthocyanin pigmentation are functionally conserved among plant species and have distinct sets of target genes. Plant Cell. 1993;5(11):1497–512.
17. Zhang H, Koes R, Shang H, Fu Z, Wang L, Dong X, Quattrocchio FM. Identification and functional analysis of three new anthocyanin R2R3-MYB genes in Petunia. Plant Direct. 2019;3(1):e00114.
18. Jiu S, Guan L, Leng X, Zhang K, Haider MS, Yu X, Fang J. The role of VvMYBA2r and VvMYBA2w alleles of the MYBA2 locus in the regulation of anthocyanin biosynthesis for molecular breeding of grape (*Vitis* spp.) skin coloration. Plant Biotechnol J. 2021;19(6):1216–39.
19. Ban Y, Honda C, Hatsuyama Y, Igarashi M, Bessho H, Moriguchi T. Isolation and functional analysis of a MYB transcription factor gene that is a key regulator for the development of red coloration in Apple skin. Plant Cell Physiol. 2007;48(7):958–70.
20. Wang XC, Wu J, Guan ML, Zhao CH, Geng P, Zhao Q. Arabidopsis MYB4 plays dual roles in flavonoid biosynthesis. Plant J. 2020;101(3):637–52.
21. Zhu L, Shan H, Chen S, Jiang J, Gu C, Zhou G, Chen F. The heterologous expression of the chrysanthemum R2R3-MYB transcription factor CmMYB1 alters lignin composition and represses flavonoid synthesis in *Arabidopsis Thaliana*. PLoS ONE. 2013;8(6):e65680.

22. Yoshida K, Ma D, Constabel CP. The MYB182 protein down-regulates Proanthocyanidin and anthocyanin biosynthesis in Poplar by repressing both structural and regulatory flavonoid genes. Plant Physiol. 2015;167(3):693–710.
23. Petroni K, Tonelli C. Recent advances on the regulation of anthocyanin synthesis in reproductive organs. Plant Sci. 2011;181(3):219–29.
24. Naing AH, Kim CK. Roles of R2R3-MYB transcription factors in transcriptional regulation of anthocyanin biosynthesis in horticultural plants. Plant Mol Biol. 2018;98(1):1–18.
25. Li X, Cao L, Jiao B, Yang H, Ma C, Liang Y. The bHLH transcription factor AcB2 regulates anthocyanin biosynthesis in onion (*Allium Cepa* L). Hortic Res. 2022.
26. Al-Snafi AE. Medical importance of cichorium intybus–A review. IOSR J Pharm. 2016;6(3):41–56.
27. Perović J, Šaponjac VT, Kojić J, Krulj B, Moreno DA, García-Viguera C, Bodroža-Solarov M, Ilić N. Chicory (*Cichorium intybus* L.) as a food ingredient–Nutritional composition, bioactivity, safety, and health claims: A review. Food Chem. 2021;336:127676.
28. Lei T, Huang J, Ruan H, Qian W, Fang Z, Gu C, Zhang N, Liang Y, Wang Z, Gao L, Wang Y. Competition between FLS and DFR regulates the distribution of flavonols and proanthocyanidins in rubus Chingii Hu. Front Plant Sci. 2023;14:1134993.
29. Shaipulah NFM, Muhlemann JK, Woodworth BD, Van Moerkercke A, Verdonk JC, Ramirez AA, Haring MA, Dudareva N, Schuurink RC. *CCoAOMT* down-regulation activates anthocyanin biosynthesis in Petunia. Plant Physiol. 2016;170(2):717–31.
30. Rao MJ, Duan M, Yang M, Fan H, Shen S, Hu L, Wang L. Novel insights into anthocyanin metabolism and molecular characterization of associated genes in sugarcane rinds using the metabolome and transcriptome. Int J Mol Sci. 2021;23(1):338.
31. Meng Y, Zhang H, Fan Y, Yan L. Anthocyanins accumulation analysis of correlated genes by metabolome and transcriptome in green and purple peppers (*Capsicum annuum*). BMC Plant Biol. 2022;22(1):358.
32. Lu J, Zhang Q, Lang L, Jiang C, Wang X, Sun H. Integrated metabolome and transcriptome analysis of the anthocyanin biosynthetic pathway in relation to color mutation in miniature roses. BMC Plant Biol. 2021;21(1):257.
33. Lang X, Li N, Li L, Zhang S. Integrated metabolome and transcriptome analysis uncovers the role of anthocyanin metabolism in Michelia maudiae. Int J Genomics. 2019;2019(1):4393905.
34. Sunil L, Shetty NP. Biosynthesis and regulation of anthocyanin pathway genes. Appl Microbiol Biotechnol. 2022;106(5):1783–98.
35. Su W, Tao R, Liu W, Yu C, Chen J. Characterization of four polymorphic genes controlling red leaf colour in lettuce that have undergone disruptive selection since domestication. Plant Biotechnol J. 2020.
36. Chen Y, Wu P, Zhao Q, Tang Y, Chen Y, Li M, Jiang H, Wu G. Overexpression of a phosphate starvation response AP2/ERF gene from physic nut in Arabidopsis alters root morphological traits and phosphate starvation-induced anthocyanin accumulation. Front Plant Sci. 2018;9:1186.
37. Liu CC, Chi C, Jin LJ, Zhu J, Yu JQ, Zhou YH. The bZIP transcription factor HY5 mediates CRY1a-induced anthocyanin biosynthesis in tomato. Plant Cell Environ. 2018;41(8):1762–75.
38. An JP, Yao JF, Xu RR, You CX, Wang XF, Hao YJ. Apple bZIP transcription factor MdbZIP44 regulates abscisic acid-promoted anthocyanin accumulation. Plant Cell Environ. 2018;41(11):2678–92.
39. Zhou H, Lin-Wang K, Wang H, Gu C, Dare AP, Espley RV, He H, Allan AC, Han Y. Molecular genetics of blood-fleshed Peach reveals activation of anthocyanin biosynthesis by NAC transcription factors. Plant J. 2015;82(1):105–21.
40. Sun Q, Jiang S, Zhang T, Xu H, Fang H, Zhang J, Su M, Wang Y, Zhang Z, Wang N, Chen X. Apple NAC transcription factor MdNAC52 regulates biosynthesis of anthocyanin and Proanthocyanidin through MdMYB9 and MdMYB11. Plant Sci. 2019;289:110286.
41. Zhang S, Chen Y, Zhao L, Li C, Yu J, Li T, Yang W, Zhang S, Su H, Wang L. A novel NAC transcription factor, MdNAC42, regulates anthocyanin accumulation in red-fleshed Apple by interacting with MdMYB10. Tree Physiol. 2020;40(3):413–23.
42. Meng Y, Bai Y, Chen D, Ma T, Si W, Yuan Y, Chen L, Zhou Y. Integration of transcriptome and metabolome reveals key regulatory mechanisms affecting sepal color variation in *Aquilegia oxysepala*. Sci Hort. 2024;334:113334.
43. Cai H, Zhang M, Chai M, He Q, Huang X, Zhao L, Qin Y. Epigenetic regulation of anthocyanin biosynthesis by an antagonistic interaction between H2A.Z and H3K4me3. New Phytol. 2019;221(1):295–308.
44. Shen F, He H, Huang X, Deng Y, Yang X. Insights into the convergent evolution of Fructan biosynthesis in angiosperms from the highly characteristic Chicory genome. New Phytol. 2023;238(3):1245–62.
45. Maroufi A, Van Bockstaele E, De Loose M. Validation of reference genes for gene expression analysis in Chicory (*Cichorium intybus*) using quantitative real-time PCR. BMC Mol Biol. 2010;11:1–12.

Publisher's note